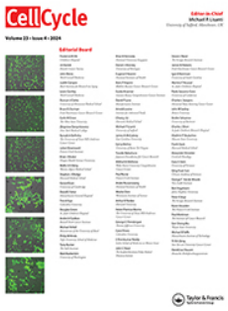

Cell Cycle

ISSN: (Print) (Online) Journal homepage: www.tandfonline.com/journals/kccy20

Knock down of APE1 suppressed gastric cancer metastasis via improving immune disorders caused by myeloid-derived suppressor cells

Baoming Zhang, Qiang Tang, Wenchao Shi, Zengtao Bao, Shanting Gao & Cheng Pan

To cite this article: Baoming Zhang, Qiang Tang, Wenchao Shi, Zengtao Bao, Shanting Gao & Cheng Pan (08 May 2024): Knock down of APE1 suppressed gastric cancer metastasis via improving immune disorders caused by myeloid-derived suppressor cells, Cell Cycle, DOI: 10.1080/15384101.2024.2351629

To link to this article: https://doi.org/10.1080/15384101.2024.2351629

CELL CYCLE
https://doi.org/10.1080/15384101.2024.2351629

Knock down of APE1 suppressed gastric cancer metastasis via improving immune disorders caused by myeloid-derived suppressor cells

Baoming Zhang[a,b,c], Qiang Tang[a,b,c], Wenchao Shi[a,b,c], Zengtao Bao[a,b,c], Shanting Gao[a,b,c], and Cheng Pan[a,b,c]

[a]Gastrointestinal Surgery Department, The First People's Hospital of Lianyungang, Lianyungang, Jiangsu, China; [b]Gastrointestinal Surgery Department, Lianyungang Clinical Medical College, Nanjing Medical University, Lianyungang, Jiangsu, China; [c]Gastrointestinal Surgery Department, Lianyungang Hospital Affiliated to Xuzhou Medical University, Lianyungang, Jiangsu, China

ABSTRACT

Gastric cancer is a highly immunogenic malignancy. Immune tolerance facilitated by myeloid-derived suppressor cells (MDSCs) has been implicated in gastric cancer resistance mechanisms. The potential role of APE1 in regulating gastric cancer metastasis by targeting MDSCs remains uncertain. In this study, the plasmid Plxpsp-mGM-CSF was used to induce high expression of granulocyte-macrophage colony-stimulating factor (GM-CSF) in GES-1 cells. For tumor transplantation experiments, AGS, AGS+GM-CSF and AGS+GM-CSF-siAPE1 cell lines were established by transfection, followed by subcutaneous implantation of tumor cells. MDSCs, Treg cells, IgG, CD3 and CD8 levels were assessed. Transfection with siAPE1 significantly inhibited tumor growth compared to the AGS+GM-CSF group. APE1 gene knockdown modulated the immune system in gastric cancer mice, characterized by a decrease in MDSCs and an increase in Treg cells, IgG, CD3 and CD8. In addition, APE1 gene knockdown resulted in decreased levels of pro-MDSC cytokines (HGF, CCL5, IL-6, CCL12). Furthermore, APE1 gene knockdown inhibited proliferation, migration and invasion of AGS and MKN45 cells. AGS-GM-CSF cell transplantation increased MDSC levels and accelerated tumor growth, whereas APE1 knockdown reduced MDSC levels, inhibited tumor growth and attenuated inflammatory infiltration in gastric cancer tissues. Strategies targeting the APE1/MDSC axis offer a promising approach to the prevention and treatment of gastric cancer, providing new insights into its management.

ARTICLE HISTORY
Received 24 January 2024
Revised 20 March 2024
Accepted 4 April 2024

KEYWORDS
Gastric cancer; MDSCS; APE1; AGS; tumor immune

1. Introduction

Gastric cancer stands out as one of the most prevalent malignancies globally, characterized by elevated morbidity and mortality rates [1]. Its etiology is predominantly associated with factors such as infection, diet, environment, and heredity. Treatment modalities for gastric cancer encompass surgical interventions, chemotherapy, radiotherapy, and targeted therapy [2]. Unfortunately, the early diagnosis rate for gastric cancer remains suboptimal, leading to a considerable number of patients being diagnosed at advanced stages, precluding timely surgical intervention [3]. Advanced gastric cancer management typically involves a combination of traditional radiotherapy, chemotherapy, and targeted therapy. Regrettably, this approach is marked by a grim prognosis, poor tolerability, substantial adverse reactions, and a low survival rate [4].

The pathogenesis of gastric cancer is intricately linked to various cells within the tumor microenvironment – a multifaceted and dynamic milieu comprising tumor cells, immune cells, such as cancer-associated fibroblasts, mesenchymal stem cells, endothelial cells, M2 tumor-associated macrophages, myeloid-derived suppressor cells (MDSCs), regulatory T cells, cytokines, and other small molecules [5,6]. MDSCs, characterized as a heterogeneous group of undifferentiated mature myeloid cells exhibiting granulocytic, immunosuppressive, and monocytic features, play a pivotal role in gastric cancer progression [7]. Upon the onset of gastric cancer, MDSCs can be induced to proliferate and accumulate in the tumor site through the vascular system, becoming integral components of the tumor microenvironment [8]. MDSCs, by secreting chemokines, cytokines, and

CONTACT Baoming Zhang 790020230057@xzhmu.edu.cn Gastrointestinal Surgery Department, The First People's Hospital of Lianyungang, No. 6 Zhenhua East Road, Lianyungang, Jiangsu Province 222061, China
Supplemental data for this article can be accessed online at https://doi.org/10.1080/15384101.2024.2351629

enzymes, exert immunosuppressive functions, facilitating immune escape. This, in turn, amplifies tumor cell proliferation, survival, adhesion, invasion, thereby fostering tumor progression and metastasis [9].

Apurinic/apyrimidinic endonuclease-reduction /oxidation factor 1 (APE1) is a versatile biological enzyme with significant roles in DNA repair and redox signaling pathways [10]. It exerts widespread influence on tumorigenesis, development, as well as responses to chemotherapy, radiotherapy, and targeted therapy through its redox regulation of nucleic acid endonucleases and transcription factors [11]. Aberrant expression of APE1 has been identified in various malignant tumors, including hepatocellular carcinoma, where studies have linked its elevated expression to the proliferation and apoptosis of hepatocellular carcinoma cells [12].

However, the potential impact of APE1 on gastric cancer malignancy, particularly through its modulation of MDSCs and downstream molecules, remains unclear. In this study, we employed Plxpsp-mGM-CSF transfection to in vivo stimulate an increase in MDSCs. Tumor transplantation experiments were conducted using AGS, AGS +GM-CSF, and AGS+GM-CSF-siAPE1 cell lines. Our results demonstrate that APE1 knockdown not only impedes tumor progression but also alleviates inflammatory infiltration within gastric cancer tissues. This highlights the significance of the APE1/MDSC axis in gastric cancer pathogenesis. Strategies targeting this axis emerge as promising avenues for both the prevention and treatment of gastric cancer, providing novel insights into the management of gastric cancer.

2. Materials and methods

2.1. Cell culture

In this study, GES-1 (#IM-H084, Immocell, China), AGS (#CRL-1739, ATCC, US), MKN45 (#IM-H088, Immocell, China), MKN28 (#IM-H294, Immocell, China) and KATO III (HTB-103, ATCC, US) cells were used in this research. These cells were cultured in Dulbecco's modified Eagle's medium (DMEM, Gibco, #12491015, US) supplemented with 5% fetal bovine serum (FBS, #26010066, Gibco, US), 50 μg/ml streptomycin (#ST487, Beyotime, China) and 50 IU penicillin (#V900929, Sigma, US). Cells were maintained in a humidified incubator at 37°C with 5% CO_2.

2.2. Cell transfection

GES-1 cells were transfected with Plxpsp-mGM-CSF using Lipofectamine 3000 (#L3000001, Invitrogen, US) for 48 hours. Plxpsp-mGM-CSF contains the granulocyte-macrophage colony-stimulating factor (GM-CSF) gene and confers resistance to hygromycin B (200 μg/mL). The supernatant from transfected GES-1 cells containing the Plxpsp-mGM-CSF gene was then applied to AGS cells for 48 hours, resulting in the designation of these cells as AGS+GM-CSF. si-APE1 (20 nM) was used to transfect AGS or AGS+GM-CSF for 48 hours, resulting in the designation of AGS +siAPE1 and AGS+GM-CSF+siAPE1, respectively.

2.3. Establishment of a mouse gastric cancer model

AGS (2×10 [7], 0.1 ml), AGS+GM-CSF (2×10 [7], 0.1 ml) or AGS+GM-CSF-siAPE1 (2×10 [7], 0.1 ml) cells were injected subcutaneously into the dorsal side of severe combined immunodeficiency (SCID) mice (SPF grade, 5 weeks old, 20–25 g). All animal experiments were ethically approved by the Ethics Committee of Fujian Medical University Affiliated Fujian Provincial Hospital.

2.4. Immunohistochemical staining (IHC)

After animal sacrifice, spleens were collected, dehydrated, embedded in paraffin and sectioned at 10 μm. Antigen retrieval was achieved by microwave heating for 3 minutes followed by incubation in 3% hydrogen peroxide for 3 minutes. The sections were then washed with PBS, blocked with 5% skim milk (#MB4219–3, meilunbio) and incubated with primary antibodies. Subsequent steps included three washes, 4 hours secondary antibody incubation, DAB staining (#P0203, Beyotime, China), dehydration and mounting. Observations were made with an Olympus B×41microscope (Tokyo, Japan). The antibodies used in IHC were listed as follows.

Rabbit monoclonal to CD3 antibody (#ab16669, Abcam, UK), Rabbit monoclonal to CD8 antibody (#ab217344, Abcam, UK). In the negative control group, we used PBS instead of primary antibody. We quantified tissue staining intensity using Image J software. The staining intensity values of all groups were subtracted from the staining intensity values of the negative control group. The AGS group was used as an experimental control and the staining intensity values of this group were homogenized. The staining intensity values of the other groups were compared to the AGS group. Then, statistical analysis among different groups was performed.

2.5. Flow cytometry

Blood samples (200 μL) were collected from the eyes at week 3, and flow cytometry analysis was performed using FITC-labeled CD3 (#11-0032-82, Invitrogen, US) and CD8 (#ab210367, Abcam, UK) monoclonal antibodies.

2.6. Measurement of IgG and GM-CSF

Peripheral blood samples were collected three weeks after tumor implantation and the levels of IgG (#ab151276, Abcam, UK) and GM-CSF (#BMS612, Invitrogen, US) were measured quantitatively by enzyme-linked immunosorbent assay (ELISA). The sensitivity of IgG ELISA kit is 1 ng/mL, and the R^2 of standard curve was 0.989. The sensitivity of GM-CSF ELISA kit is 2 pg/mL, and the R^2 of standard curve was 0.991.

2.7. Measurement of MDSCs and Treg cells

Three weeks after tumor implantation, blood samples were collected for enucleation. Peripheral blood mononuclear cell suspension was prepared using the Percoll method. CD3+ lymphocytes were isolated using anti-CD3 magnetic beads, and CD8+ T lymphocytes were sorted by flow cytometry. The remaining fluid was separated using magnetic beads and flow cytometry to isolate CD11b+ MDSCs. Data analysis was performed using BD CELL Quest software.

2.8. CCK8 assay

Cells in the logarithmic growth phase were washed with PBS, digested with trypsin, suspended in serum-free culture medium and adjusted to a cell concentration of 1×10 [5]/ml. These cells were then cultured in a 96-well plate for 24 hours. After incubation with CCK8 reagent (Beyotime, #C0038, China) for 2 hours, absorbance at 450 nm was detected. A blank control was used with wells containing corresponding amounts of cell culture medium and CCK-8 reagent but without cells added. The si-NC group was used as the experimental control.

2.9. Transwell assay

A total of 2×10 [6] cells were seeded in the upper chamber with Matrigel (diluted 1:3, #356234, Corning, US) and serum-free medium. The bottom chamber contained DMEM with 10% FBS (#26010066, Gibco, US). After 48 hours, invasive cells in the lower chamber were fixed with 4% methanol and stained with crystal violet (#C0775, Sigma-Aldrich, US).

2.10. Wound healing assay

For the wound healing assay, cells were digested with trypsin (#108444, Sigma-Aldrich, US), centrifuged and seeded in a 6-well plate at a density of 1×10 [6] cells per well. After reaching 90% confluence in the cell culture incubator for 24 hours, the cell monolayer was scratched using a 200 μL pipette tip. After two washes with PBS to remove non-adherent cells, the gap left by the scratch was clearly visible. Fresh serum-free culture medium was added and the distance between the wounds was measured at 0 and 24 hours, followed by migration distance analysis.

2.11. Bioinformatic analysis

Gene expression and survival analyses were performed using GEPIA (http://gepia.cancer-pku.cn/) and TCGA (https://www.cancer.gov/about-nci/organization/ccg/research/structural-genomics/tcga). RNA purity and integrity were assessed using a NanoPhotometer spectrophotometer and

an Agilent 2100 Bioanalyzer, respectively. Library construction was performed using the NEBNext® Ultra™ RNA Library Prep Kit for Illumina. Sequencing was performed using the synthetic sequencing method and StringTie (version 1.3.3b) was used for novel gene prediction. Differential expression analysis for two comparison groups was performed using DESeq2 software, with adjusted p values and |log2foldchange| as significance thresholds.

2.12. Western blotting

Proteins were lysed using RIPA lysis buffer (#R0278, Sigma, US) containing a protein phosphatase inhibitor. Protein concentration was determined by the BCA method (#A045-4-1, Nanjing Jiancheng Bioengineering Institute, Nanjing, China) and equal amounts of protein were loaded on 10% SDS-PAGE gels. Proteins were then transferred to a PVDF membrane (Milipore, #GVWP02500, US). After blocking with 5% skim milk in TBST (Beyotime, #P0222, China) for 3 hours, the membranes were incubated with primary antibodies overnight at 4°C, followed by incubation with secondary antibodies for 3 hours at room temperature. Target gene detection was performed using an enhanced chemiluminescence detection kit from Thermo Fisher (#32132, US), and ImageJ software was used for band analysis. The antibodies used in western blotting were listed as follows. Rabbit polyclonal to GAPDH (#ab9485, Abcam, UK), Rabbit monoclonal to APE1 (#ab92744, Abcam, UK), and Goat anti-rabbit IgG antibody (#ab6721, Abcam, UK).

2.13. RT-PCR

For RT-PCR analysis, RNA was extracted from tissues using Trizol (#R0016, Beyotime). RNA purity was assessed using a NanoPhotometer spectrophotometer (Thermo Scientific, USA). Reverse transcription was performed using the Takara PrimeScript RT Reagent Kit with gDNA Eraser Kit (#RR047A). RT-PCR amplification was performed using the Bio-Rad C×F96system. The relative expression level of the target gene was determined using the $2^{-\Delta\Delta CT}$ method. GAPDH expression was used as for normalization.

2.14. Statistical analysis

Data are expressed as mean ± standard deviation. Statistical analyses were performed using SPSS software version 18. A p value less than 0.05 was considered statistically significant, and statistical analysis included t-tests and analysis of variance.

3. Results

3.1. Differential expression of APE1 in gastric cancer

Using the GEPIA and TCGA databases, we performed an analysis of APE1 expression in different tumor types and found significant differences in its expression between tumor and normal tissues. Notably, gastric cancer tissues showed a significant decrease in APE1 expression (Figure 1(a,b)). The reduced expression of APE1 correlated negatively with tumor stage (Figure 1(c)) and positively with higher survival rates (Figure 1(d)). In addition, APE1 expression was significantly lower in normal gastric cells (Figure 1(e)).

3.2. Overexpression of GM-CSF in AGS and inhibitory effects of siAPE1 on tumor growth

GES-1 cells were transfected with Plxpsp-mGM-CSF (f)or 48 hours, resulting in a significant increase in GM-CSF expression in the supernatant (Figure 2(a)). Culturing AGS cells with the GM-CSF-rich supernatant resulted in a significant increase in both intracellular and extracellular GM-CSF levels (Figure 2(b, c)). Thus, successful establishment of AGS cells with enhanced GM-CSF expression was achieved. Subsequent transfection with siAPE1 resulted in the establishment of AGS+GM-CSF-siAPE1 cells. In addition, the transfection efficiency of si-APE1 was confirmed (Figure 2(d)) with RT-PCR. The si-APE1 was shown to reduce target gene expression by around 75% 48 hours post transfection. Compared to the AGS+GM-CSF group, siAPE1 transfection significantly inhibited tumor growth (Figure 2(e)).

3.3. APE1 knockdown modulates the immune system in gastric tumor mice

Compared to the AGS group, the AGS+GM-CSF group showed a significant increase in MDSC

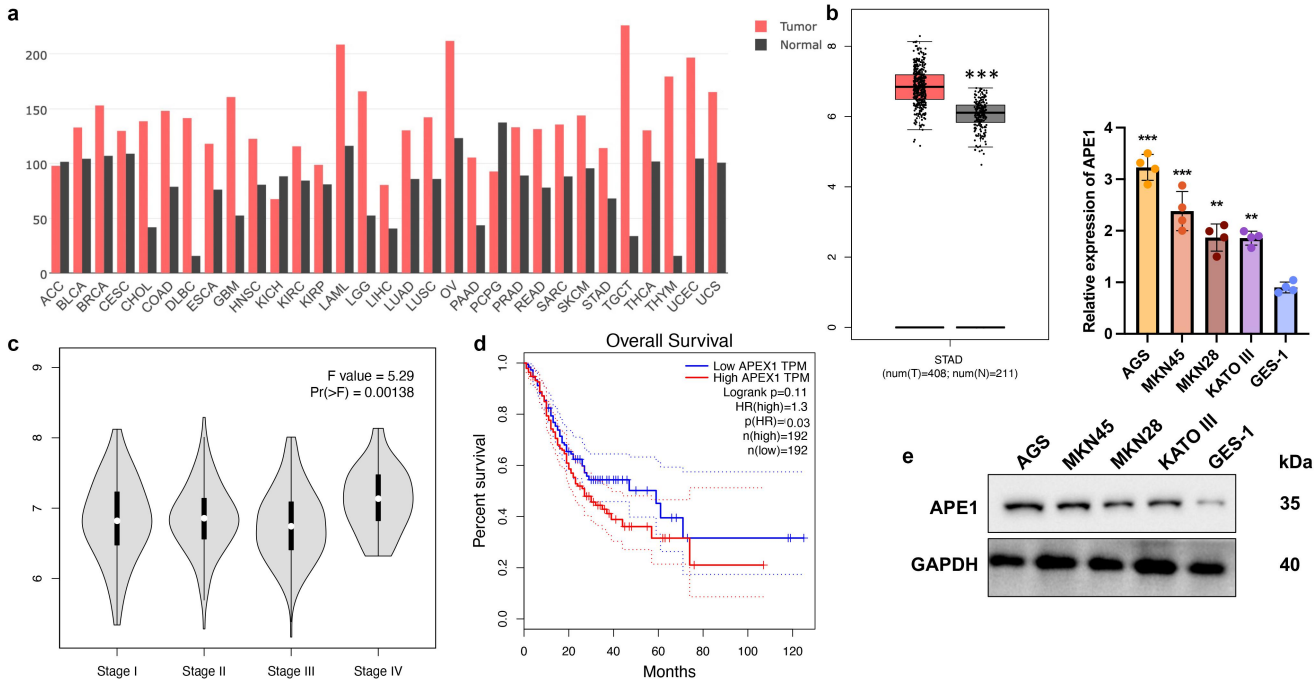

Figure 1. Differential expression of APE1 in gastric cancer. APE1 expression was analyzed in various tumor types and normal tissues using GEPIA and TCGA databases (A-B). Based on GEPIA analysis, decreased APE1 expression was negatively correlated with tumor stage and positively correlated with higher survival rate (C-D). APE1 expression in cancer cells and tissues was measured by Western blotting and IHC staining (E-F). The statistical significance was indicated as $^{**}p < 0.01$ and $^{***}p < 0.001$.

levels (Figure 3(a)). However, MDSCs were significantly suppressed in the AGS+GM-CSF-siAPE1 group. Furthermore, lower levels of Treg cells and IgG were observed in the AGS+GM-CSF group, but these indicators were significantly increased in the AGS+GM-CSF-siAPE1 group (Figure 3(b,c)). In addition, GM-CSF levels increased in the AGS+GM-CSF group but decreased after siAPE1 treatment (Figure 3(d)). CD3 and CD8 levels in peripheral blood and spleen tissues were reduced in the AGS+GM-CSF group, but siAPE1 transfection significantly increased CD3 and CD8 levels (Figure 4(a,b)). These results suggest that AGS+GM-CSF transplantation promotes tumor growth and suppression of the immune system, whereas siAPE1 transfection inhibits tumor development and enhances the immune system.

3.4. APE1 knockdown enhances anti-tumor immunity in subcutaneous AGS mouse model

Gene expression profiling comparisons revealed an enrichment of immune and inflammatory response pathways in the AGS+GM-CSF-siAPE1 group compared to the AGS+GM-CSF group (Figure 5(a,b)). SiAPE1 treatment resulted in the downregulation of key genes associated with MDSC accumulation, such as CCL2 and CCL17 (Figure 5(c)). RT-qPCR analysis of isolated gastric tumor tissues confirmed lower levels of pro-MDSC cytokines (HGF, CCL5, IL-17, CCL17 and IL7R) in the AGS+GM-CSF-siAPE1 group (Figure 5(d)). KEGG pathway analysis revealed significant enrichment in the inflammatory response, cytokine activity and hypoxia pathways in the AGS +GM-CSF-siAPE1 treatment group compared to the AGS+GM-CSF group (Figure 5(e,f)).

3.5. APE1 knockdown suppresses AGS and MKN45 cell viability

SiAPE1 significantly inhibited invasion, proliferation and migration of AGS and MKN45 cells compared to the si-NC treatment group (Figure 6 (a-c)). Furthermore, APE1 depletion resulted in a significant increase in apoptosis compared to the si-NC treatment group (Figure 6(d)). These results further confirm the tumor suppressive effects of siAPE1.

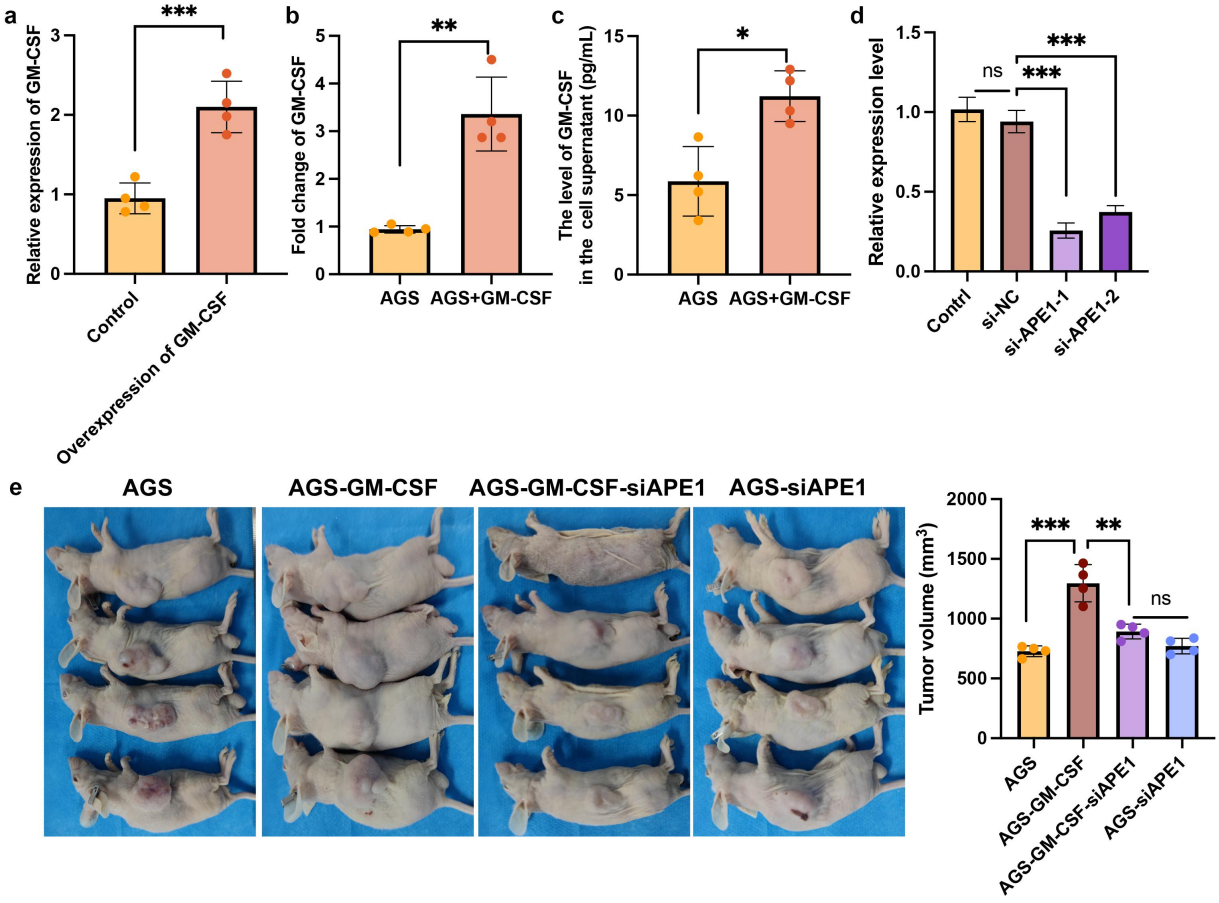

Figure 2. GM-CSF overexpression in AGS and tumor growth suppression by siAPE1. (A) Establishment of high GM-CSF expression in HBE cells ($n = 4$); (B) significant GM-CSF expression in cells after incubation with supernatant containing high levels of GM-CSF ($n = 4$); (C) high GM-CSF expression in supernatant after incubation with supernatant containing high levels of GM-CSF ($n = 4$); (D) the transfection efficiency of si-APE1 was confirmed with RT-PCR. (E) Inhibition of tumor growth by siAPE1 transfection compared with AGS+GM-CSF group. $^{**}p < 0.01$, $^{***}p < 0.001$.

4. Discussion

Gastric cancer stands out as one of the most prevalent and globally significant tumors. According to the International Agency for Research on Cancer in 2020, it held the fifth position in terms of incidence and the fourth position in mortality rates worldwide [13]. Due to its elusive onset, a considerable number of gastric cancer patients receive their diagnosis at an advanced stage, highlighting the urgency for effective detection methods [14]. Presently, chemoradiotherapy remains the primary treatment modality for advanced gastric cancer, with molecular targeting and immunotherapy providing extensions to patient survival [15]. However, even with radical surgery, chemoradiotherapy faces challenges such as a high recurrence and metastasis rate, diminished quality of life, a low 5-year survival rate, and significant toxic side effects [16]. Consequently, addressing these issues has become a focal point in advancing the treatment of advanced gastric cancer.

MDSCs are overexpressed in both primary and metastatic solid tumors, intricately linked to tumor development and progression [17]. Functioning as a heterogeneous group of undifferentiated and mature myeloid progenitor cells, MDSCs impede the normal differentiation process under sustained low-intensity stimulation from tumors, inflammation, and other pathological conditions [18]. This arrested differentiation manifests in different stages, conferring immune-suppressive functions. Not only do MDSCs enable tumors to evade immune surveillance, but they also significantly contribute to tumor metastasis [19]. Their involvement extends beyond the regulation of anti-tumor immune function, impacting the survival and growth of

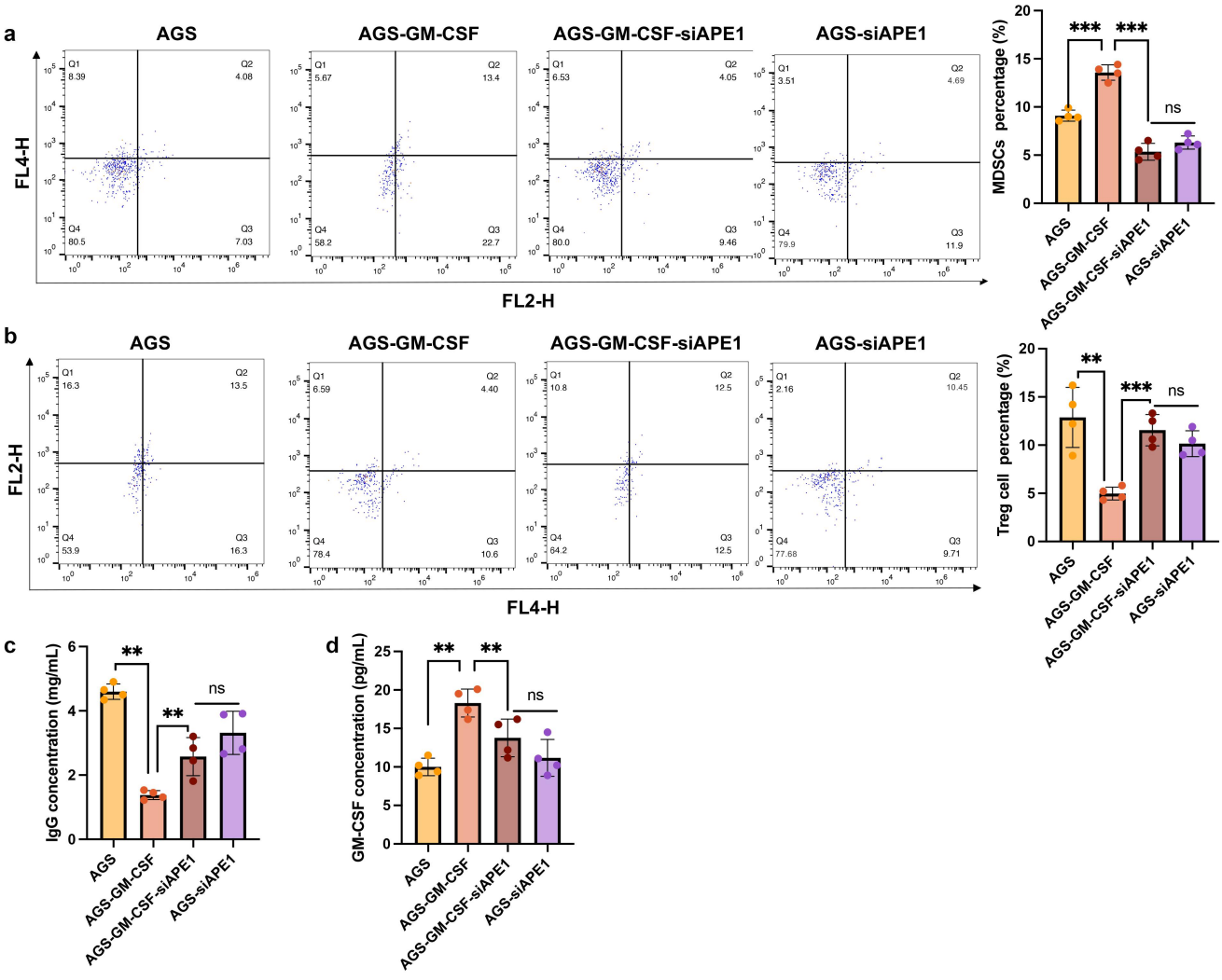

Figure 3. Knockdown of APE1 regulated the immune system of gastric tumor mice. (A) Significant inhibition of MDSCs in the AGS +GM-CSF-siAPE1 group compared to AGS+GM-CSF; (B) analysis of Treg cells by flow cytometry; (C) analysis of IgG levels by ELISA; (D) analysis of GM-CSF levels. *$p < 0.05$, **$p < 0.01$, ***$p < 0.001$.

cancer cells, promoting epithelial-mesenchymal transition, and facilitating metastasis [20]. Cytokines secreted by MDSCs, such as CCL2, CXCL12, and CXCL5, synergize with tumor cells, inducing malignant transformation, recruiting MDSCs, and fostering metastasis to tumor sites [21]. In tumor tissue, MDSCs rapidly differentiate into tumor associated macrophages, and this phenomenon was related to the downregulation of STAT3 activity, which is controlled by the activation of CD45 phosphatase induced by hypoxia [22]. The endoplasmic reticulum stress response pathway is associated with the inhibitory activity of MDSCs [23]. Transcription factor CHOP is associated with MDSC suppressive activity at the tumor site. CHOP-deficient MDSC lose the ability to suppress T cells stimulated in an antigen-nonspecific manner [24]. å

In this study, the induction of GM-CSF overexpression was observed to stimulate a significant increase in MDSCs. Notably, the heightened MDSCs in the AGS+GM-CSF group were markedly suppressed upon siAPE1 intervention (Figure 3(a)). Furthermore, APE1 knockdown orchestrated a modulation of the immune system in gastric tumor mice, characterized by a reduction in MDSCs and an augmentation of Treg cells, IgG, CD3, and CD8 (Figures 3 and 4).

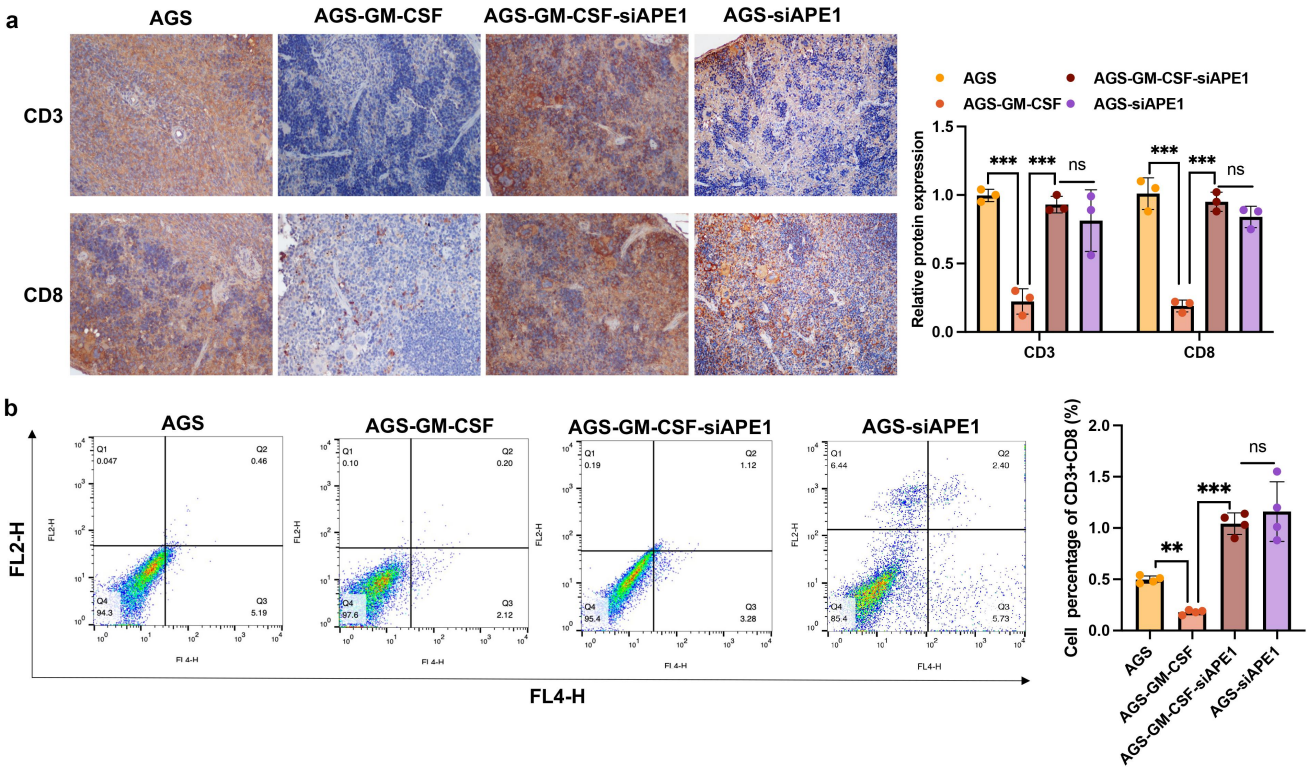

Figure 4. APE1 knockdown enhances CD3+ and CD8+ levels. (A) Analysis of CD3+ and CD8+ cells by flow cytometry; (B) analysis of CD3+ and CD8+ cells by IHC staining. $^{**}p < 0.01$, $^{***}p < 0.001$.

The DNA damage repair function of APE1, coupled with the regulation of crucial transcription factors, plays a pivotal role in various aspects of chemotherapy resistance [25]. APE1 exhibits high expression in diverse malignant tumor tissues, and this heightened expression is correlated with chemoresistance [26]. In this research, a cell line with APE1 knockdown was established to elucidate the role of APE1 in regulating MDSCs derived from gastric cancer. The differential genes between the AGS+GM-CSF and AGS+GM-CSF-siAPE1 groups were systematically screened and validated (Figure 5 (a–d)). The observed suppression of MDSCs-produced chemokines (HGF, CCL5, IL-17, CCL17, and IL-17 R) by siAPE1 underscores the potential of APE1 as a highly promising therapeutic target for cancer treatment.

However, there are some limitations in this study. (1) More clinical data need to be integrated to validate our conclusions. (2) We did not identify an in-depth mechanism for the role of APE1 in regulating MDSCs during gastric cancer development.

5. Conclusion

Transplantation of AGS-GM-CSF led to an increase in MDSC levels, which contributed to accelerated tumor growth. Conversely, reduction of MDSCs by APE1 knockdown effectively inhibited tumor progression and attenuated inflammatory infiltration in gastric cancer tissues. Strategies targeting the APE1/MDSC axis represent a novel avenue for the prevention and treatment of gastric cancer.

List of abbreviations

Myeloid-derived suppressor cells (MDSCs), Granulocyte-macrophage colony-stimulating factor (GM-CSF), Apurinic/apyrimidinic endonuclease-reduction/oxidation factor 1 (APE1), Severe combined immunodeficiency (SCID), Immunohistochemical staining (IHC), Enzyme-linked immunosorbent assay (ELISA).

Disclosure statement

No potential conflict of interest was reported by the author(s).

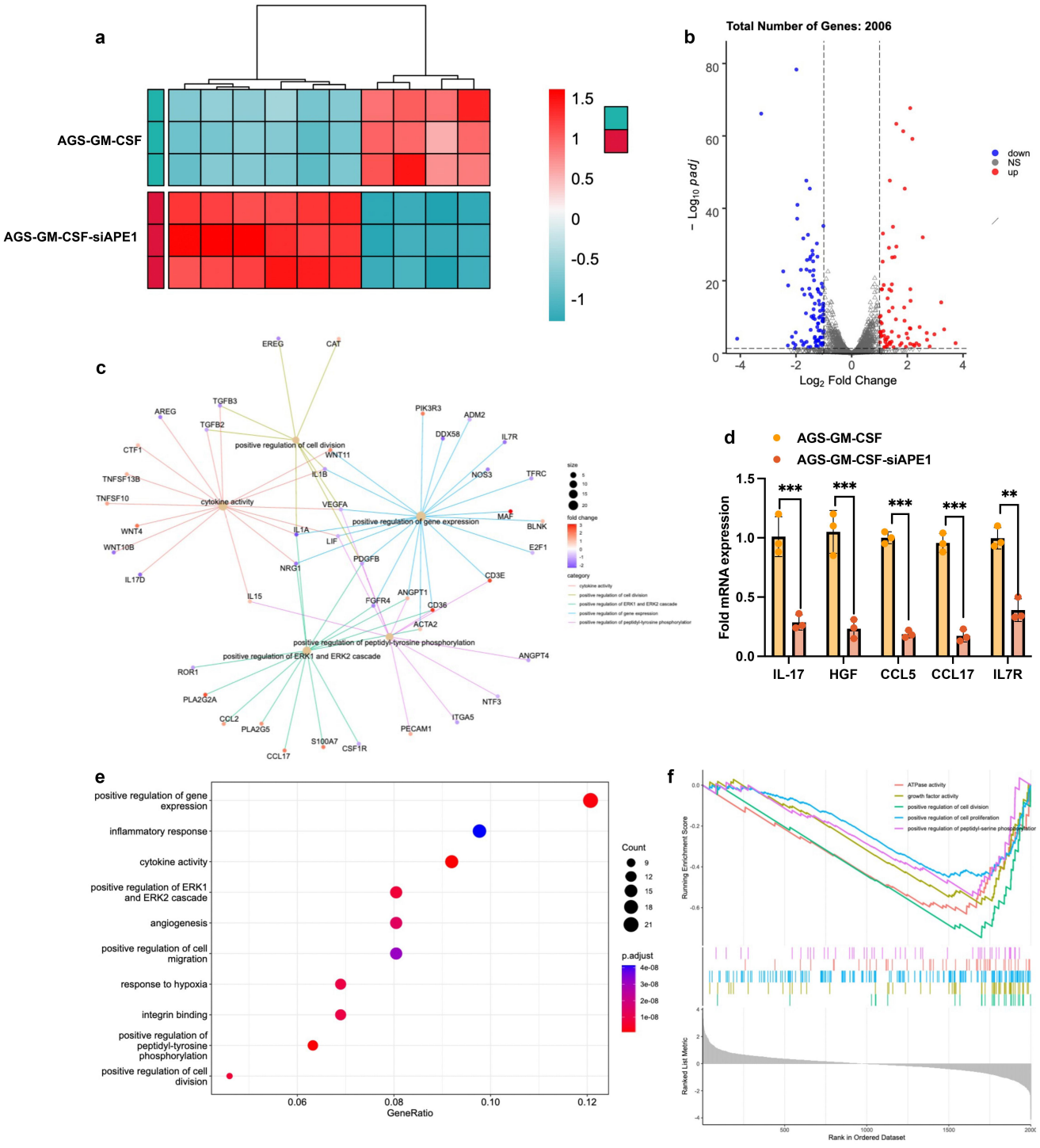

Figure 5. APE1 knockdown enhances anti-tumor immunity in subcutaneous AGS mouse model. (A) PCA analysis; (B-C) differential expression gene analysis; (D) KEGG pathway analysis; (E) validation of MDSC-related cytokine expression by RT-PCR; (F) summary of transcriptome analysis. $^{**}p < 0.01$, $^{***}p < 0.001$.

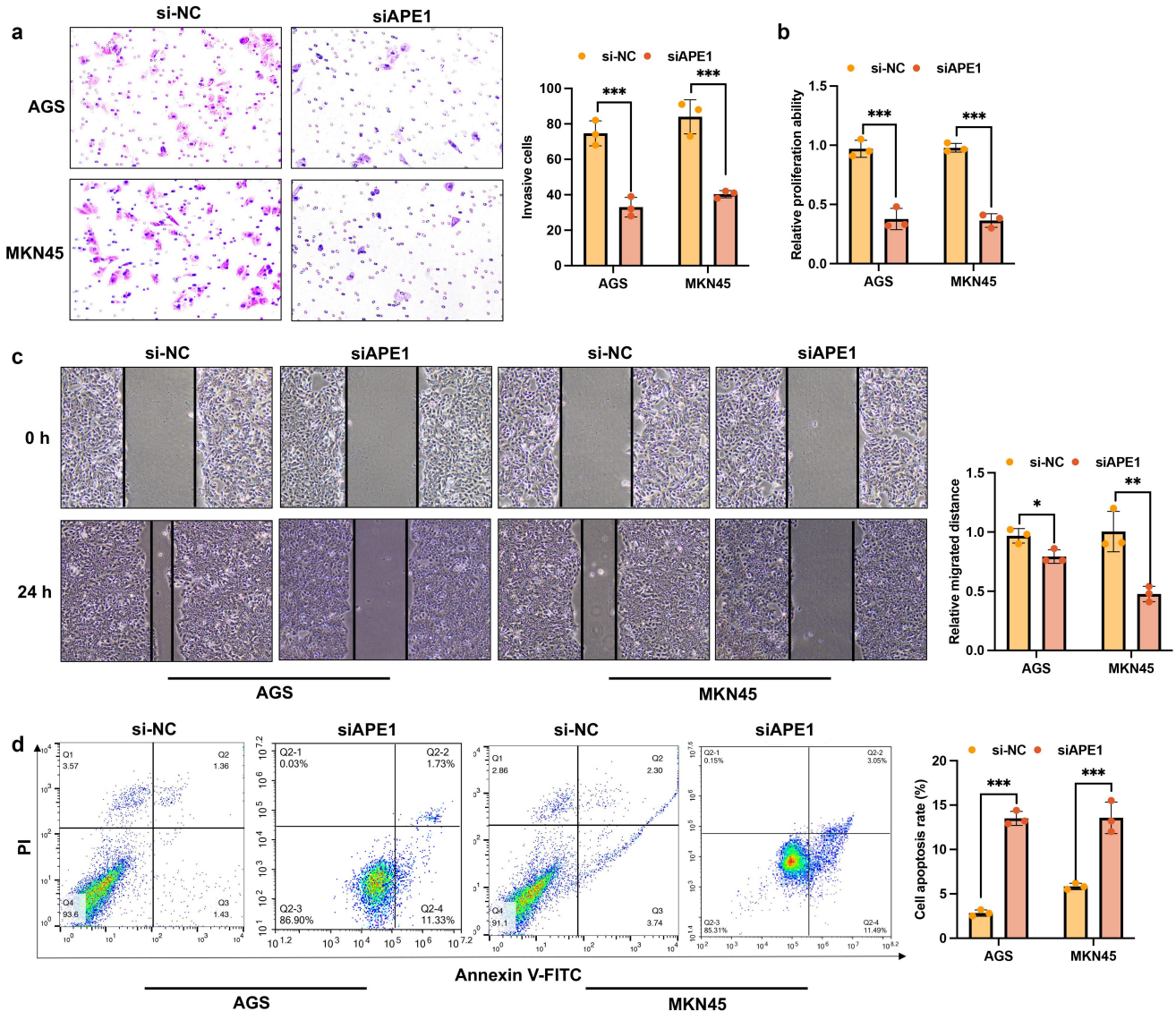

Figure 6. APE1 knockdown inhibits cell viability in AGS and MKN45 cells. (A-D) (A-D) detection of cell invasion, proliferation, migration, and apoptosis by Transwell, CCK8, wound healing, and flow cytometry assays. $^{**}p < 0.01$, $^{***}p < 0.001$.

Funding

This work was supported by Doctor Scientific Research Start Fund Project of the First People's Hospital of Lianyungang [Grant Nos. BS1902] and the Program of Medical Technology of the First People's Hospital of Lianyungang [Grant Nos.XJ1912].

Authors' contributions

BZ conceived and designed the experiments; QT, WS, ZB, SG, and CP performed the experiments; BZ wrote the paper. All authors approved for this submission.

Ethical Approval and Consent to participate

Ethical approval was obtained from the institutional ethics committee of The First People's Hospital of Lianyungang

Availability of data and material

The data and material used to support the findings of this study are included within the manuscript, and the RNA-seq data was uploaded to GEO data base (GSE262050).

References

[1] Tsutsumi C, Ohuchida K, Katayama N, et al. Tumor-infiltrating monocytic myeloid-derived suppressor cells contribute to the development of an immunosuppressive tumor microenvironment in gastric cancer. Gastric Cancer. 2024;27(2):248–262. doi: 10.1007/s10120-023-01456-4

[2] Kao KD, Grasberger H, El-Zaatari M. The Cxcr2(+) subset of the S100a8(+) gastric granylocytic myeloid-derived suppressor cell population (G-MDSC) regulates gastric

pathology. Front Immunol. 2023;14:1147695. doi: 10.3389/fimmu.2023.1147695

[3] Chen Y, Liu J, Chen Y, et al. Jianpi Yangzheng Xiaozheng decoction alleviates gastric cancer progression via suppressing exosomal PD-L1. Front Pharmacol. 2023;14:1159829. doi: 10.3389/fphar.2023.1159829

[4] Liu Y, Wei D, Deguchi Y, et al. PPARδ dysregulation of CCL20/CCR6 axis promotes gastric adenocarcinoma carcinogenesis by remodeling gastric tumor microenvironment. Gastric Cancer. 2023;26(6):904–917. doi: 10.1007/s10120-023-01418-w

[5] Tang Y, Zhou C, Li Q, et al. Targeting depletion of myeloid-derived suppressor cells potentiates PD-L1 blockade efficacy in gastric and colon cancers. Oncoimmunology. 2022;11(1):2131084. doi: 10.1080/2162402X.2022.2131084

[6] Ding L, Chakrabarti J, Sheriff S, et al. Toll-like receptor 9 pathway mediates Schlafen(+)-MDSC Polarization During Helicobacter-induced Gastric Metaplasias. Gastroenterology. 2022;163(2):411–25 e4. doi: 10.1053/j.gastro.2022.04.031

[7] Zhou X, Fang D, Liu H, et al. PMN-MDSCs accumulation induced by CXCL1 promotes CD8(+) T cells exhaustion in gastric cancer. Cancer Lett. 2022;532:215598. doi: 10.1016/j.canlet.2022.215598

[8] Kodach LL, Peppelenbosch MP. Targeting the myeloid-derived suppressor cell compartment for inducing responsiveness to immune checkpoint blockade is best limited to specific subtypes of gastric cancers. Gastroenterology. 2021;161(2):727. doi: 10.1053/j.gastro.2021.03.047

[9] Kim HD, Ryu MH, Yoon S, et al. Clinical implications of neutrophil-to-lymphocyte ratio and MDSC kinetics in gastric cancer patients treated with ramucirumab plus paclitaxel. Chin J Cancer Res. 2020;32(4):621–630. doi: 10.21147/j.issn.1000-9604.2020.05.07

[10] Zhang Y, Sun M, Xie J, et al. Dual-signal amplification strategy based on Catalytic Hairpin Assembly and APE1-assisted amplification for high-contrast miRNA imaging in living cells. Anal Chem. 2024;96(2):910–916. doi: 10.1021/acs.analchem.3c05013

[11] Siqueira PB, de Sousa Rodrigues MM, de Amorim ISS, et al. The APE1/REF-1 and the hallmarks of cancer. Mol Biol Rep. 2024;51(1):47. doi: 10.1007/s11033-023-08946-9

[12] Gautam A, Fawcett H, Burdova K, et al. APE1-dependent base excision repair of DNA photodimers in human cells. Mol Cell. 2023;83(20):3669–78 e7. doi: 10.1016/j.molcel.2023.09.013

[13] Korbecki J, Bosiacki M, Barczak K, et al. The clinical significance and role of CXCL1 chemokine in gastrointestinal cancers. Cells. 2023;12(10):12. doi: 10.3390/cells12101406

[14] Liu X, Yan C, Yang A, et al. Efficacy of anti-programmed cell death protein 1 monoclonal antibody combined with bevacizumab and/or Pseudomonas aeruginosa injection in transplanted tumor of mouse forestomach carcinoma cell gastric cancer in mice and its mechanism in regulating tumor immune microenvironment. Clin Exp Immunol. 2023;213(3):328–338. doi: 10.1093/cei/uxad069

[15] Ding L, Sheriff S, Sontz RA, et al. Schlafen4(+)-MDSC in Helicobacter-induced gastric metaplasia reveals role for GTPases. Front Immunol. 2023;14:1139391. doi: 10.3389/fimmu.2023.1139391

[16] Chen Y, Chen Y, Tan S, et al. Visual analysis of global research on immunotherapy for gastric cancer: a literature mining from 2012 to 2022. Human Vaccines Immunother. 2023;19(1):2186684. doi: 10.1080/21645515.2023.2186684

[17] Kim W, Chu TH, Nienhuser H, et al. PD-1 signaling promotes tumor-infiltrating myeloid-derived suppressor cells and gastric tumorigenesis in mice. Gastroenterology. 2021;160(3):781–796. doi: 10.1053/j.gastro.2020.10.036

[18] Liu M, Zhang Y, Chen L, et al. Myeloid-derived suppressor cells in gastroenteropancreatic neuroendocrine neoplasms. Endocrine. 2021;71(1):242–252. doi: 10.1007/s12020-020-02467-2

[19] Yamaguchi T, Fushida S, Kinoshita J, et al. Extravasated platelet aggregation contributes to tumor progression via the accumulation of myeloid-derived suppressor cells in gastric cancer with peritoneal metastasis. Oncol Lett. 2020;20(2):1879–1887. doi: 10.3892/ol.2020.11722

[20] Tavukcuoglu E, Horzum U, Yanik H, et al. Human splenic polymorphonuclear myeloid-derived suppressor cells (PMN-MDSC) are strategically located immune regulatory cells in cancer. Eur J Immunol. 2020;50(12):2067–2074. doi: 10.1002/eji.202048666

[21] Fabian KP, Padget MR, Donahue RN, et al. PD-L1 targeting high-affinity NK (t-haNK) cells induce direct antitumor effects and target suppressive MDSC populations. J Immunother Cancer. 2020;8(1):e000450. doi: 10.1136/jitc-2019-000450

[22] Corzo CA, Condamine T, Lu L, et al. HIF-1α regulates function and differentiation of myeloid-derived suppressor cells in the tumor microenvironment. J Exp Med. 2010;207(11):2439–2453. doi: 10.1084/jem.20100587

[23] Condamine T, Kumar V, Ramachandran IR, et al. ER stress regulates myeloid-derived suppressor cell fate through TRAIL-R–mediated apoptosis. J Clin Invest. 2014;124(6):2626–2639. doi: 10.1172/JCI74056

[24] Condamine T, Gabrilovich DI. Can the suppressive activity of myeloid-derived suppressor cells Be "Chop"ped? Immunity. 2014;41(3):341–342. doi: 10.1016/j.immuni.2014.08.016

[25] Lu H, Cao LL, Ballout F, et al. Reflux conditions induce E-cadherin cleavage and EMT via APE1 redox function in oesophageal adenocarcinoma. Gut. 2023;73(1):47–62. doi: 10.1136/gutjnl-2023-329455

[26] Tao J, Zhang H, Weinfeld M, et al. Development of a DNAzyme walker for the detection of APE1 in living cancer cells. Anal Chem. 2023;95(40):14990–14997. doi: 10.1021/acs.analchem.3c02574